ChemComm

COMMUNICATION

View Article Online
View Journal | View Issue

Cite this: *Chem. Commun.*, 2021, **57**, 3123

Received 25th December 2020,
Accepted 25th January 2021

DOI: 10.1039/d0cc08346a

rsc.li/chemcomm

Two-photon induced isomerization through a cyaninic molecular antenna in azo compounds†

Emmanuel Villatoro,[a] Leonardo Muñoz-Rugeles,[a] Jesús Durán-Hernández,[a] Bernardo Salcido-Santacruz,[a] Nuria Esturau-Escofet,[a] Jose G. López-Cortés,[a] M. Carmen Ortega-Alfaro[b] and Jorge Peón*[a]

We present a new design for non-linear optically responsive molecules based on a modular scheme where a polymethinic antenna section with important two-photon absorption properties is bonded to an isomerizable actuator section composed of a stilbenyl-azopyrrole unit. Upon two photon excitation, energy migration from the antenna-localized second singlet excited state to the stilbenyl-azopyrrole section allows for efficient indirect excitation and phototransformation of this actuator.

Reactive response to light is inspiring new molecular control schemes with applications in photo-pharmacology,[1] catalytic process initiation, and the manipulation of molecular gears.[2] The initial step in these processes is an electronic excitation which triggers a specific molecular transformation.[1,2] For many of these applications, it is crucial to have high spatial control of the photochemistry. Such control can be achieved if the initial excitation occurs by a non-linear absorption event.

In this contribution, a new bichromophoric design for non-linear optically switchable molecules is proposed. The main idea is to use two chromophores to isolate the two-photon absorption (2PA) properties in one section (the antenna), and the photochemical transformation in another segment (the actuator) as seen in Scheme 1. The moieties are joined through an ether type functionality in a way that the two keep their independent properties as localized chromophores.[3] In this design, upon 2PA at the antenna, the energy associated with the excitation is used to efficiently drive changes in the actuator region after rapid exciton migration.

The actuator in our design is a π-extended stilbenil-azopyrrole (SAP). Azoheteroarenes have shown outstanding properties as photoswitches, providing a versatile scaffold for future applications. Also, from their extended conjugation, they have transition energies appropriate for indirect excitation through energy transfer from specific upper states in the antenna section (see below).[4] In our design, the antenna is the polymethinic IR780 cyanine dye. Its symmetry properties make the S_0 to S_2 transition strongly two-photon allowed (with 460 GM units at 860 nm).[5]

Scheme 1 outlines the relevant energy levels for our design and proposed mechanism. The S_2 polymethinic state (formed by 2PA) requires a long enough lifetime for the exciton migration to occur before internal conversion to the S_1 state within this chromophore. The large energy gap between the S_2 and the S_1 cyaninic states (of about 1.0 eV), results in a small vibronic coupling. Thus, for this kind of cyanines, the S_2 lifetime can be in the time scale of picoseconds.[5]

Scheme 2 displays an overview of the synthetic method. Briefly, a Mirozoki–Heck cross-coupling between **1** and **2** affords the intended SAP actuator. To accomplish this coupling, it was crucial the use of complex **3** as catalytic precursor.[6] A nucleophilic reaction couples SAP through an ether bond to the IR780 cyanine rendering the expected Cy-SAP system. Detailed synthesis and characterization for the SAP and Cy-SAP molecules are included in the ESI.†

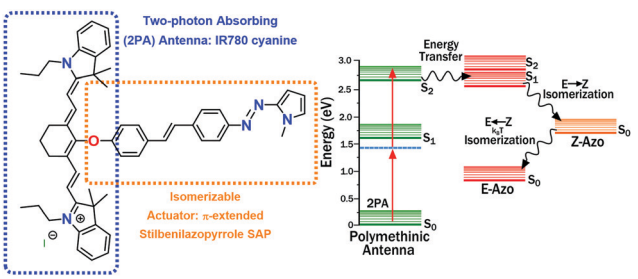

Scheme 1 Molecular structure of the Cy-SAP dyad. Relative energy diagram of the electronic levels for the polymethinic "two-photon antenna" based on the IR780 cyanine, coupled to a stilbenyl-azopyrrolic (SAP) actuator.

[a] *Instituto de Química, Universidad Nacional Autónoma de México, Ciudad de México, Mexico. E-mail: jpeon@unam.mx*

[b] *Instituto de Ciencias Nucleares, Universidad Nacional Autónoma de México, Ciudad de México, Mexico*

† Electronic supplementary information (ESI) available: Synthesis and characterization of CySAP. Experimental and computational details. Time-resolved spectral data for individual components. See DOI: 10.1039/d0cc08346a

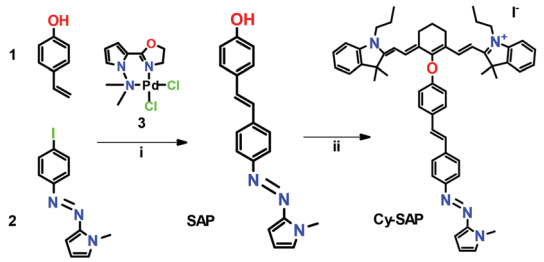

Scheme 2 Synthetic methodology. (i) 0.1% of **3**, DMF, 160 °C, 2 h. (ii) **IR780**, Et_3N, MeCN, r.t., 24 h.

The key design element of the Cy-SAP system relies on its modular structure. The chromophores keep their respective electronic transition patterns despite the covalent linkage. As seen in Fig. 1, the Cy-SAP absorption spectrum replicates the merged spectrum formed by the simple sum of the SAP and IR780 spectra. From the match, it can be concluded that the SAP unit and the cyaninic section of Cy-SAP keep their excited singlet manifold order and character. The latter is crucial for our design as the cyanine keeps its symmetry and state ordering properties. These properties are essential for a large two-photon absorption cross-section into its S_n ($n > 1$) states.[5]

Polymethine chromophores have been shown to produce significant emissions from their S_2 singlet.[5a] Fig. 1 shows the well-defined emission band from IR780's S_2 state at 528 nm. This well-defined emission results from the remarkably slow decay of this upper singlet state of several cyanines compared to that of other common chromophores.[5a] As stated above, our scheme is based on energy transfer coupling between the two sections. Thus, it requires the presence of isoenergetic electronic transitions. Such energy matching will involve the S_2 state of the antenna with the first excited state of the acceptor (SAP). The spectral overlap is shown in the inset of Fig. 1.

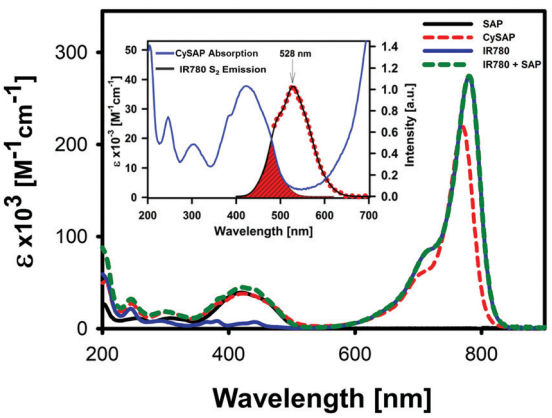

Fig. 1 Absorption spectrum of Cy-SAP (dashed red line) and, for comparison, the sum of the absorption spectra of SAP and IR780 (dashed green line). We also include the absorption spectra of SAP (black line) and IR780 (blue line). Inset: Absorption spectrum of Cy-SAP and emission spectrum from the second excited singlet state of the IR780 cyanine. All spectra were taken in acetonitrile. The red area indicates the spectral overlap between the FRET pair. Fig. S7 in the ESI,† confirms that this emission band results from electronic excitation of the cyanine into its S_n ($n > 1$) states.

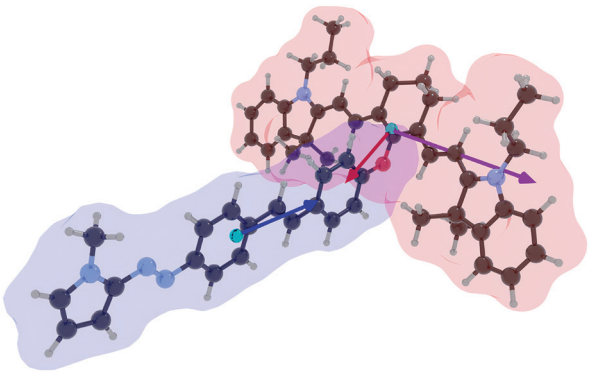

Fig. 2 Calculated equilibrium geometry of Cy-SAP. The red area shows the biphotonic antenna and the blue section highlights the isomerizable actuator. The arrows indicate the transition dipole moments where the blue vector corresponds to the first transition localized in SAP, the purple vector corresponds to the first transition localized in the antenna section, and the red vector corresponds to the second transition localized in the antenna ($S_2 \rightarrow S_0$).

TD-DFT calculations at the PBE0//M06 6-311++G(d,p) (PCM = CH_3CN) level of theory were performed to estimate the energy transfer parameters.[7] The relevant transition moments are depicted in Fig. 2 and are shown within the optimized Cy-SAP structure. The IR780 antenna S_2 state bears an emission transition vector oriented along the short molecular axis in the direction of the *meso* substituent. The SAP actuator has a strong $S_0 \rightarrow S_1$ transition dipole oriented along its main axis and towards the antenna. These vectors are nearly collinear and correspond to a high orientation factor, κ^2, for energy transfer: 3.76 (for PBE0) and 3.73 (for the M06 functional).

Our estimation of the coupling between the two chromophores of Cy-SAP considers a Förster mechanism.[8] The parameters include the spectral overlap shown in Fig. 1, the orientation factor taken from our TD-DFT calculations, and the experimental lifetime of the cyaninic S_2 state in IR780. Further details are found in the ESI.† The predicted antenna to actuator energy transfer yield is between 75.0% (PBE0) and 74.8% (M06). Such large yield for transfer from the S_2 state localized at the antenna section to the S_1 state localized at the actuator comes from four main factors: (1) a favourable κ^2 orientation factor, (2) a large oscillator strength for the acceptor transition of 4×10^4 M^{-1} cm^{-1}, (3) a long-lived upper singlet state for the cyanine-localized S_2 donor singlet state of 1.45 ps (see below), and (4) the proximity of the chromophores of 0.92 nm (center to center).

The photochemical transformation of the actuator of Cy-SAP was first studied by direct linear excitation of the SAP unit within Cy-SAP and compared against the behaviour of the isolated actuator SAP. The results are summarized in Table 1. Upon irradiation, the Cy-SAP system rapidly evolves towards a photo-stationary state (PSS). Fig. 3 shows the complete thermal back isomerization. NMR spectroscopy of the PSS shows a clear mixture of *E* and *Z* isomers as seen in the inset of Fig. 3. A complete and clean thermal isomerization back to the *E* isomer was observed within several minutes for both molecules. The corresponding data for SAP is included in Fig. S14 (ESI†).

Table 1 Isomerization parameters for SAP and Cy-SAP

	$t_{1/2}$[a] [min]	k[a] [s^{-1}]	PSS[b] [%] E	PSS[b] [%] Z	$\Phi_{E\rightarrow Z}$[c] [%]
Cy-SAP	5.5	7.2×10^{-4}	56	44	22 ± 2
SAP	5.5	6.8×10^{-4}	32	68	29 ± 1

[a] For the first-order $Z \rightarrow E$ back thermal isomerization. [b] Method described by Calbo *et al.*[4a] [c] Method proposed by Börjesson.[9] A 10^{-5} M acetonitrile solution and a 485 nm continuous laser were used to obtain the photostationary state.

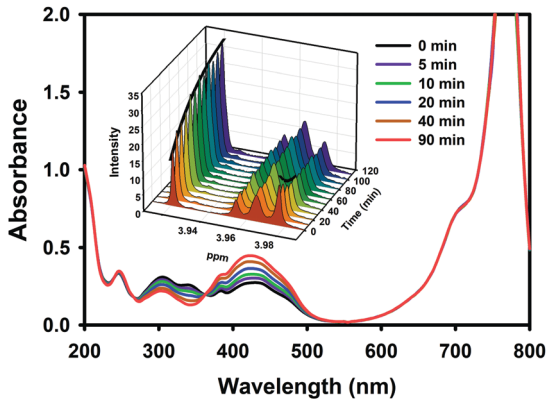

Fig. 3 Thermal Z–E back-isomerization was observed after the formation of a photo-stationary state in Cy-SAP solutions. Main: UV-Vis kinetics. Inset: ^{1}H NMR spectroscopy kinetics. The spectrum shown is a section of the complete spectrum shown in Fig. S15 in the ESI.†

The PSS spectra of SAP and Cy-SAP were deconvoluted into their E and Z components in Fig. S16 (ESI†). The E/Z ratio in the PSS of Cy-SAP is only slightly smaller than that in SAP. Furthermore, Fig. S18 (ESI†) indicates that both systems are capable of several switching cycles without any noticeable fatigue. Such photo-conversion properties are significant and appropriate for several kinds of applications.[1]

The fact that the isomerization quantum yield in going from SAP to Cy-SAP only shows a small drop is quite relevant. The indirect non-linear excitation of the stilbenyl-azopyrrole section is to occur by energy transfer from a higher antenna-localized excited state. However, a cyaninic lower energy state (S_1, 780 nm band) is present and could provide deactivation channel due to back energy transfer (actuator back to cyanine). The minor $E \rightarrow Z$ yield drop (from 0.29 to 0.22) implies that this not a predominant pathway. Therefore, this potential drawback does not impede the photochemistry in the actuator section.

The main advantage of the Cy-SAP system is its control through non-linear excitation with NIR light. Focused laser pulses tuned to energies slightly below the first cyaninic transition (860 nm) induce the corresponding isomerization. Fig. 4 depicts the resulting spectral evolution after 2PA. The $E \rightarrow Z$ photoinduced response of the system is identical to that observed for linear photoisomerization with visible light in Fig. 3. The clear isosbestic point at 365 nm shown in Fig. 4 and the complete thermal back-isomerization in Fig. S21 (ESI†)

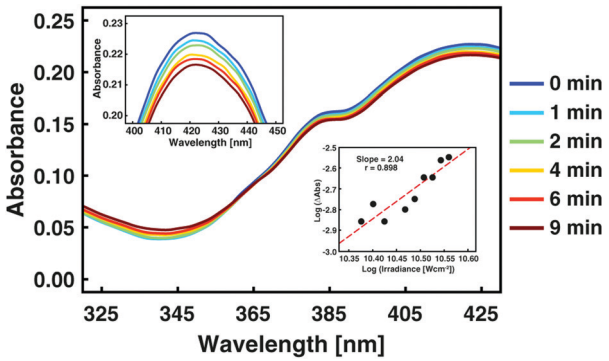

Fig. 4 Evolution from the E-isomer to the Z isomer of Cy-SAP as a function of irradiation time. The electronic excitation in these experiments corresponds to two-photon absorption of 860 nm, 100 fs laser pulses. The experimental details are included in the ESI.† The lower inset shows the square dependence of the transformation as a function of pulse intensity.

demonstrate a clean two-photon isomerization. Experiments at different excitation powers show no photodegradation at the powers of the experiments (see Fig. S19, ESI†). Back-to-back tests with the SAP molecule (without the antenna) showed no evolution at the same conditions and corroborate the essential role of the antenna section. Given the biphotonic nature of the excitation, the PSS shows a smaller E–Z transformation for this PSS in the overall volume of the cell (see Fig. S19, ESI†). However, this is not a concern since these systems are meant for applications where the effects are microscopically localized, like in organelles or liposomes, where localized single molecule photo-transformations are crucial[1d,2] (rather than large bulk effects).

Femtosecond-resolved fluorescence measurements were used to directly observe the mechanistic aspects of the antenna S_2 excitation and energy migration in Cy-SAP. Biphotonic fluorescence up-conversion is ideal for these characterizations since transient emissions from higher states can be resolved in the sub-ps scale. Fig. S23 (ESI†) displays the detection of the emission from the upper excited states of Cy-SAP. Experiments detecting the emissions from the isolated antenna (IR780) and actuator (SAP) are depicted in the ESI,† in Fig. S23.

The emission intensities of Fig. S23 (ESI†) correspond to the energy region of the spontaneous emission from the cyaninic-localized S_2 state. These signals exhibit a single exponential decay of 200 ± 60 fs for the Cy-SAP system. These decays are much faster in comparison with those from the S_2 emission for the IR780 (antenna-only) case, which is congruent with the proposed mechanism. Specifically, the IR780 emission in Fig. S23 (ESI†) shows a bi-exponential decay with time constants of 220 fs and 1.45 ps due to $S_2 \rightarrow S_1$ internal conversion, where the sub-ps dynamics are attributed to fast relaxation events after excitation. The lack of the 1.45 ps component in Cy-SAP indicates that system evolves into the energy-transfer state before the population of the relaxed cyaninic S_2 state is established. The initial (near $t = 0$) emission spectrum of Cy-SAP resembles that of the IR780 cyanine in Fig. S23 (ESI†) indicating the nature of the originally excited state. However,

the Cy-SAP traces decay much faster and display the formation of a shoulder at shorter wavelengths corresponding to the emission from the SAP excited states shown in Fig. S23 (ESI†). The faster signal loss in Fig. S23 (ESI†) is consistent with the presence of a new channel for the evolution of the cyanine-localized state (polymethinic S_2), due to the presence of the antenna-to-actuator energy migration channel, indicated as "energy transfer" in Scheme 1.

Kinetic modeling of the emission signals agrees with the observed changes between IR780 Cy-SAP. The population modeling used follows the proposed mechanism and is described in the ESI.† The model accounts for the changes in the up-conversion signals considering a Förster type energy transfer rate constant from the S_2 state.

Besides the sub-ps spectral evolutions, time-resolved emission polarization anisotropies ($r(t)$) from the up-conversion signals are presented as part of the ESI.† The near time-zero ($r(t \approx 0)$) anisotropies of IR780, SAP and Cy-SAP show clear differences. Here, Cy-SAP shows a significantly smaller $r(0)$ value than the IR780 and SAP solutions. This low anisotropy is consistent with the presence of the additional S_2 decay channel in Cy-SAP from exciton migration (see ESI†).

It should be noticed that the emission decays and anisotropies from Cy-SAP in the 475 to 600 nm region are due to: two-photon excitation into a superposition of S_n states, the "not-so-rapid" internal conversion to the cyaninic S_1 state of approximately $k_{IC} \approx 10^{12}$ s^{-1}, and exciton migration to form the SAP localized excited states. Our femtosecond experiments show clear differences between the dynamics of the separate fragments (IR780 and SAP) and those of the antenna-actuator system Cy-SAP, which are consistent with the mechanism indicated in Scheme 1.

In summary, the absorbance changes due to the *E–Z* isomerization as a function of the 860 nm excitation intensity in Fig. 4 demonstrate the biphotonic nature of this transformation. Crucial back-to-back tests with SAP show no isomerization evidence at these powers for the actuator-only solutions or IR780 – SAP mixtures. Such experiments demonstrate that the CySAP non-linear isomerization response requires the presence of the antenna section. The cyaninic moiety provides the 2PA properties in this modular design where actuator excitation occurs indirectly. The Cy-SAP molecule represents a proof of concept for this general design where the antenna section provides the actuator with significant two-photon properties using a near-resonant step-like transition (cyaninic S_1 at 1.5 eV) to augment the 2PA properties of NIR light. This modular design and the resulting non-linear properties can have applications in areas where highly localized *E–Z* photoisomerization processes are important, including the de-stabilization of liposomes for content-release, and the control of *cis–trans* isomerization related to macromolecular control, or photopharmacological schemes.[10]

Authors acknowledge CONACyT-México grant Ciencia de Frontera 2019-51496, CONACyT-México 285722, and PAPIIT/DGAPA/UNAM IG200621 for financial support, DGTIC-UNAM project LANCAD-UNAM-DGTIC-210 for computer time.

Conflicts of interest

There are no conflicts to declare.

Notes and references

1 (*a*) W. A. Velema, W. Szymanski and B. L. Feringa, *J. Am. Chem. Soc.*, 2014, **136**, 2178–2191; (*b*) K. Hüll, J. Morstein and D. Trauner, *Chem. Rev.*, 2018, **118**, 10710–10747; (*c*) I. Tochitsky, M. A. Kienzler, E. Isacoff and R. H. Kramer, *Chem. Rev.*, 2018, **118**, 10748–10773; (*d*) C. Matera, A. M. J. Gomila, N. Camarero, M. Libergoli, C. Soler and P. Gorostiza, *J. Am. Chem. Soc.*, 2018, **140**, 15764–15773; (*e*) M. Wegener, M. J. Hansen, A. J. M. Driessen, W. Szymanski and B. L. Feringa, *J. Am. Chem. Soc.*, 2017, **139**, 17979–17986.

2 (*a*) R. Dorel and B. L. Feringa, *Chem. Commun.*, 2019, **55**, 6477–6486; (*b*) F. M. Raymo and M. Tomasulo, *Chem. – Eur. J.*, 2006, **12**, 3186–3193; (*c*) D. Roke, S. J. Wezenberg and B. L. Feringa, *Proc. Natl. Acad. Sci. U. S. A.*, 2018, **115**, 9423–9431.

3 (*a*) J. Moreno, M. Gerecke, L. Grubert, S. A. Kovalenko and S. Hecht, *Angew. Chem., Int. Ed.*, 2016, **55**, 1544–1547; (*b*) M. Izquierdo-Serra, M. Gascón-Moya, J. J. Hirtz, S. Pittolo, K. E. Poskanzer, È. Ferrer, R. Alibés, F. Busqué, R. Yuste and J. Hernando, *et al.*, *J. Am. Chem. Soc.*, 2014, **136**, 8693–8701; (*c*) J. Croissant, A. Chaix, O. Mongin, M. Wang, S. Clément, L. Raehm, J.-O. Durand, V. Hugues, M. Blanchard-Desce and M. Maynadier, *et al.*, *Small*, 2014, **10**, 1752–1755; (*d*) G. Cabré, A. Garrido-Charles, M. Moreno, M. Bosch, M. Porta-de-la-Riva, M. Krieg, M. Gascón-Moya, N. Camarero, R. Gelabert and J. M. Lluch, *et al.*, *Nat. Commun.*, 2019, **10**, 907.

4 (*a*) J. Calbo, C. E. Weston, A. J. P. White, H. S. Rzepa, J. Contreras-García and M. J. Fuchter, *J. Am. Chem. Soc.*, 2017, **139**, 1261–1274; (*b*) S. Crespi, N. A. Simeth and B. König, *Nat. Rev. Chem.*, 2019, **3**, 133–146; (*c*) C. E. Weston, R. D. Richardson, P. R. Haycock, A. J. P. White and M. J. Fuchter, *J. Am. Chem. Soc.*, 2014, **136**, 11878–11881.

5 (*a*) C. A. Guarin, J. P. Villabona-Monsalve, R. López-Arteaga and J. Peon, *J. Phys. Chem. B*, 2013, **117**, 7352–7362; (*b*) J. Fu, L. A. Padilha, D. J. Hagan, E. W. Van Stryland, O. V. Przhonska, M. V. Bondar, Y. L. Slominsky and A. D. Kachkovski, *J. Opt. Soc. Am. B*, 2007, **24**, 67; (*c*) R. S. Lepkowicz, O. V. Przhonska, J. M. Hales, J. Fu, D. J. Hagan, E. W. Van Stryland, M. V. Bondar, Y. L. Slominsky and A. D. Kachkovski, *Chem. Phys.*, 2004, **305**, 259–270; (*d*) J. Rodríguez-Romero, C. A. Guarin, A. Arroyo-Pieck, L. Gutiérrez-Arzaluz, R. López-Arteaga, F. Cortés-Guzmán, P. Navarro and J. Peon, *ChemPhotoChem*, 2017, **1**, 397–407.

6 (*a*) L. Muñoz-Rugeles, D. Gallardo-Rosas, J. Durán-Hernández, R. López-Arteaga, R. A. Toscano, N. Esturau-Escofet, J. G. López-Cortés, J. Peón and M. C. Ortega-Alfaro, *ChemPhotoChem*, 2020, **4**, 144–154; (*b*) F. Hochberger-Roa, S. Cortés-Mendoza, D. Gallardo-Rosas, R. A. Toscano, M. C. Ortega-Alfaro and J. G. López-Cortés, *Adv. Synth. Catal.*, 2019, **361**, 4055–4064.

7 M. J. Frisch, *et al.*, *Gaussian 09, Revision E.01*, Gaussian, Inc., Wallingford CT, 2016.

8 M. Taniguchi, H. Du and J. S. Lindsey, *Photochem. Photobiol.*, 2018, **94**, 277–289.

9 K. Stranius and K. Börjesson, *Sci. Rep.*, 2017, **7**, 1–9.

10 (*a*) D. Liu, S. Wang, S. Xu and H. Liu, *Langmuir*, 2017, **33**, 1004–1012; (*b*) M. J. Fuchter, *J. Med. Chem.*, 2020, **63**, 11436–11447; (*c*) J. Morstein, M. Awale, J. L. Reymond and D. Trauner, *ACS Cent. Sci.*, 2019, **5**, 60.

